Assessment of Langatate Material Constants and Temperature Coefficients Using SAW Delay Line Measurements

Blake T. Sturtevant, *Student Member, IEEE,* and Mauricio Pereira da Cunha, *Senior Member, IEEE*

Abstract*—This paper reports on the assessment of langatate (LGT) acoustic material constants and temperature coefficients by surface acoustic wave (SAW) delay line measurements up to 130°C. Based upon a full set of material constants recently reported by the authors, 7 orientations in the LGT plane with Euler angles (90°, 23°, Ψ) were identified for testing. Each of the 7 selected orientations exhibited calculated coupling coefficients (K^2) between 0.2% and 0.75% and also showed a large range of predicted temperature coefficient of delay (TCD) values around room temperature. Additionally, methods for estimating the uncertainty in predicted SAW propagation properties were developed and applied to SAW phase velocity and temperature coefficient of delay calculations. Starting from a purchased LGT boule, the SAW wafers used in this work were aligned, cut, ground, and polished at University of Maine facilities, followed by device fabrication and testing. Using repeated measurements of 2 devices on separate wafers for each of the 7 orientations, the room temperature SAW phase velocities were extracted with a precision of 0.1% and found to be in agreement with the predicted values. The normalized frequency change and the temperature coefficient of delay for all 7 orientations agreed with predictions within the uncertainty of the measurement and the predictions over the entire 120°C temperature range measured. Two orientations, with Euler angles (90°, 23°, 123°) and (90°, 23°, 119°), were found to have high predicted coupling for LGT ($K^2 > 0.5\%$) and were shown experimentally to exhibit temperature compensation in the vicinity of room temperature, with turnover temperatures at 50 and 60°C, respectively.

I. Introduction

Langatate (LGT, $La_3Ga_{5.5}Ta_{0.5}O_{14}$) has been considered for the past 20 years as a promising piezoelectric material for applications in frequency control, wireless communications, and sensors [1]–[9]. LGT belongs to the crystal point group 32, the same as quartz, berlinite, and gallium phosphate, and shows potential to simultaneously exhibit increased electromechanical coupling compared with quartz and temperature compensation orientations [2], [10]. Attractive properties of LGT include: 1) piezoelectric constants e_{11} and e_{14} that are 2 to 4 times higher than those of quartz; 2) the absence of phase changes and the retention of piezoelectricity up to its melting point of 1470°C; 3) high density (6147 kg/m^3); and 4) reported surface and bulk acoustic wave (SAW and BAW) orientations with temperature compensation [2], [9]–[11].

LGT orientations exhibiting temperature compensation around room temperature have previously been predicted based on published acoustic material constants [2], [11], but experimentally observed orientations of temperature compensation have occurred at temperatures up to 100°C away from room temperature [2]. Further, the literature on LGT acoustic wave (AW) material properties contains significant discrepancies regarding the values of the elastic and piezoelectric constants and their temperature coefficients as discussed in detail in [9]. It is not presently clear to what extent these discrepancies in the reported material constants and temperature coefficients arose from variations in the crystal growth parameters, composition, and material properties provided by different growers; different or imprecise measurement techniques; or some other reason yet to be determined [9], [12], [13]. In an attempt to re-examine the LGT AW constants and temperature coefficients, a carefully determined set of elastic and piezoelectric constants and temperature coefficients was recently extracted by pulse echo overlap and combined resonance techniques [9]. In that work, use was made of expansion coefficients reported in [14] and dielectric constants and respective temperature coefficients presented in [15], all performed under the same project.

The present work focuses on the assessment of these recently reported material constants and temperature coefficients by using SAW delay line devices fabricated using LGT boules originating from the same crystal supplier reported in [9], [14], [15]. Room temperature phase velocities, v_p, and temperature coefficient of delay (TCD) are extracted through S_{21} delay line frequency response measurements. The experimentally obtained v_p and TCD are then compared with those numerically predicted using the constants in [9]. Normalized frequency variations and TCD as a function of temperature are also reported in this work and compared with predictions to verify the temperature coefficients given in [9]. A method for estimating the uncertainties in the predicted v_p and TCD is developed based upon the uncertainties in the material properties, to assess the agreement between the measured and predicted v_p and TCD.

Manuscript received May 20, 2009; accepted October 14, 2009. Financial support for this work was provided in part by the Army Research Office ARO Grant #DAAD19-03-1-0117, by the Petroleum Research Fund Grant ACS PRF# 42747-AC10, by the National Science Foundation grants # ECS 0134335 and # DGE-0504494, and the Air Force Office AFO Grant # FA9550-07-1-0519.

B. T. Sturtevant is with the Department of Physics, University of Maine, Orono, ME.

M. Pereira da Cunha is with the Department of Electrical and Computer Engineering, University of Maine, Orono, ME (mdacunha@eece.maine.edu).

Digital Object Identifier 10.1109/TUFFC.2010.1444

Section II presents experimental procedures including plane selection, device fabrication, SAW phase velocity measurements, and experimental uncertainties. Section III describes how the uncertainties in the predicted SAW v_p and TCD can be estimated based on the uncertainties in the material constants. Section IV discusses the experimental results and the consistency between measurements and predictions. Finally, Section V concludes the paper.

II. Experimental Procedure

A. SAW Plane and Propagation Directions Selection

Using a full set of acoustic material constants (elastic, piezoelectric, and dielectric constants as well as density) and their respective temperature coefficients [9], [14], [15], a numerical search procedure was conducted for planes suitable for SAW evaluation. The criteria used for selecting a plane for SAW fabrication were: 1) sufficiently high electromechanical coupling (K^2) throughout plane to allow the probing of SAW propagation directions of interest within the plane; 2) that the plane exhibited a wide range of TCD, which is useful for verifying the temperature coefficients of the elastic and piezoelectric constants; and 3) use a single rotated cut or double rotated cuts with initial surface normals lying in the Y-Z, X-Z, and X-Y planes for easier alignment and maximum material usage while cutting. For the search of the crystal cut, 2 Euler angles were varied at a time in each of 3 separate searches. The 3 searches investigated the spaces defined by Euler angles: $(0°, \Theta, \Psi)$, $(90°, \Theta, \Psi)$, and $(\Phi, 90°, \Psi)$, corresponding to wafers with surface normals lying in the Y-Z, X-Z, and X-Y planes, respectively.

The plane selected for device fabrication has Euler angles $(\Phi, \Theta, \Psi) = (90°, 23°, \Psi)$, with a surface normal vector making angles of 23° and 67° with the +Z and +X axes, respectively, and a $\Psi = 0°$ propagation direction along the +Y crystalline axis. Fig. 1 shows the calculated K^2 and TCD for this plane. The plane has K^2 higher than that of ST-X quartz ($K^2 = 0.11\%$) for most of the propagation directions in the plane and exhibits K^2 close to 0.75% in a region where TCD is expected to be near zero around room temperature ($110° \leq \Psi \leq 130°$). The drop in K^2 in the vicinity of $(90°, 23°, 124°)$ is detailed in the inset of Fig. 1, which spans 20° around $\Psi = 120°$. Between $\Psi = 123°$ and 125°, K^2 reduces from 0.75% to 0.33%, because the free v_p variation is larger than the metalized v_p variation with increasing Ψ. This variation in K^2 above $\Psi = 123°$ may be relevant in device design and fabrication, in which case it should be properly considered. The 7 orientations chosen for device fabrication have predicted $K^2 > 0.2\%$, and a large range of predicted TCDs ($-64 \leq$ TCD $\leq$ 4 ppm/°C), allowing for an assessment of the previously extracted and reported elastic temperature coefficients. The 7 orientations measured in the referred plane have azimuthal angles Ψ = 0, 13, 48, 77, 119, 123, and 170° (Fig. 1).

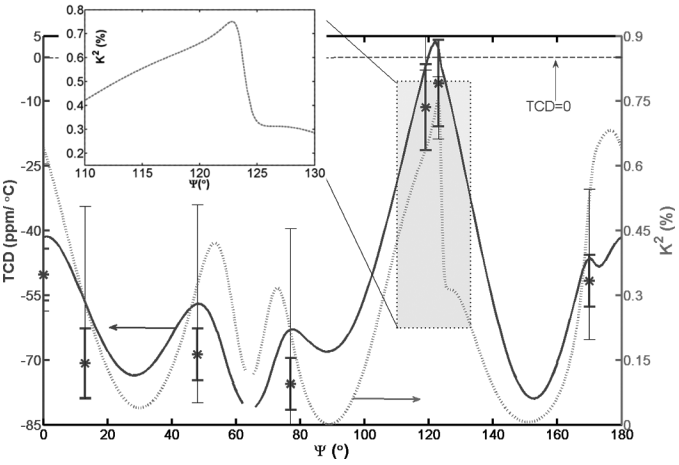

Fig. 1. Room temperature TCD (solid, left axis) and K^2 (dashed, right axis) for the plane measured (Euler angles 90°, 23°, Ψ), Ψ = 0°, 13°, 48°, 77°, 119°, 123°, and 170°. Measured TCDs are indicated with asterisks. The thin error bars correspond to the predicted TCDs. The inset details K^2 in a 20° span around $\Psi = 120°$, where this property changes significantly.

B. Device Fabrication

The wafers' alignment, cutting, grinding, polishing, and the SAW device design, fabrication, and testing were performed at the Microwave Acoustics Material Lab and Laboratory for Surface Science and Technology facilities at the University of Maine (UMaine). Wafers for SAW fabrication were cut using an inner diameter saw (Meyer-Berger, Steffisberg, Switzerland) from a Z-grown single-crystal LGT boule (Fomos Materials, Moscow, Russia), purchased around the same time as the material used for the determination of material constants reported in [9], [14], [15]. Wafers were aligned to the selected orientations to better than 6 arcminutes using a PANalytical X'Pert Pro materials research diffractometer (PANalytical, Inc., Natick, MA) using techniques described in [16] and [17]. The wafers were mechanically ground using Al_2O_3 abrasives (Micro Abrasives Corporation, Westfield, MA) of decreasing grit size down to 1 μm and then polished to an optical finish using colloidal silica (Universal Photonics, Hicksville, NY). Two identical sets of 7 SAW delay lines, shown in Fig. 2, were fabricated on the polished substrates using 1500 Å of aluminum on top of a 150 Å chromium adhesion layer. Split finger electrodes were used to reduce the triple transit response of the devices. Each finger had a width of 4 μm, yielding a SAW wavelength of $\lambda = 32$ μm at the interdigital transducer (IDT). The 7 orientations selected in the $(90°, 23°, \Psi)$ plane had predicted power flow angles (PFA) of $[-8°, -12°, 6°, 0.2°, 12.5°, -7°, 17.2°]$ for $\Psi = [0°, 13°, 48°, 77°, 119°, 123°, 170°]$, respectively. The non-zero PFAs were accounted for in the design and fabrication of delay lines. The delay lines were designed to have one transducer with an acoustic aperture of 80λ and the second transducer with an aperture of 130λ to ensure that the SAWs were measurable despite eventual variations in the PFA as a function of temperature. All transducers had

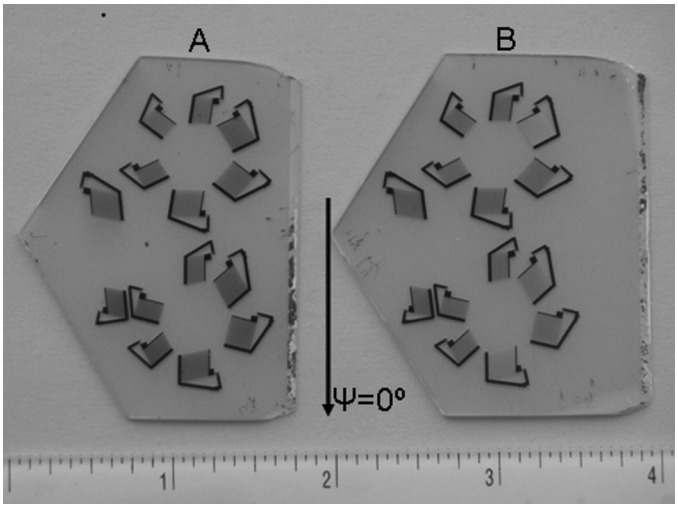

Fig. 2. The 2 wafers fabricated, each with 7 SAW delay line devices. The arrow denotes the $(90°, 23°, 0°)$ propagation direction and the ruler scale is inches.

an active length of 125λ, and the IDT center-to-center delay path was 460λ. The electrically open, mechanically unloaded delay path was chosen to be as large as possible for the prepared wafers (~3 times the length of the transducer) to minimize the influence of the electrodes on the propagation path.

C. SAW S_{21} Frequency Measurements

The S_{21} center frequency response of the devices was measured using an RF probe station (Cascade Microtech, Inc., Beaverton, OR) and an Agilent 8753 ES network analyzer (Agilent Technologies, Santa Clara, CA). Time gating was used to remove electromagnetic feed-through, residual SAW triple transit, and other spurious acoustic reflections. The gated S_{21} response was recorded and the maximum of $|S_{21}|$ was used as the center frequency for each measurement. The temperature of the devices was controlled using a Temptronic (Sharon, MA) thermal chuck with 0.1°C precision. Because of the thermal gradient between the chuck and the top surface of the LGT substrate, the temperature measured by the Temptronic controller diverges from the actual temperature of the SAW device once the thermal chuck departs from room temperature, with the discrepancy increasing with temperature. To more accurately determine the SAW operating temperature, a secondary resistance temperature device (RTD) was mounted on top of an LGT wafer of the same thickness as the device tested and used to record the temperature at the surface of the LGT substrates during all measurements. A 5°C difference between the operating temperature of the SAW and the temperature measured by the Temptronic controller was registered at 130°C.

At room temperature (25.0°C), the frequency response of each of the 14 devices (7 devices on each of 2 wafers, labeled A and B in Fig. 2) was measured 5 times to determine the precision of the frequency measurement for each device. The mean and the standard error of the frequency measurements were taken as the measured frequency, f, and the uncertainty in the measured frequency, δ_f, of each device, respectively. The SAW phase velocity, v_p, with associated uncertainty, δ_{vp}, were then calculated through the wave relationship by:

$$v_p = \lambda f, \tag{1a}$$

$$\delta_{vp} = \sqrt{\lambda^2 (\delta f)^2}, \tag{1b}$$

because the uncertainty in the photolithographically defined wavelength, λ, was considered negligible. Because the delay path consists primarily of an uncoated substrate surface, dispersion was neglected and the phase velocity calculated by (1a) was assumed to be equal to the measured group velocity.

To determine the thermal properties of the SAWs, frequency measurements were made using the 7 devices on wafer 'A' at temperatures between 10 and 130°C. The RF probe tips were lifted off of the device under test before changing the temperature to avoid destruction of the device and the probe tips caused by the thermal expansion of the LGT. The required repeated lifting off and replacement of the probe tips during the temperature runs ends up scratching away the aluminum electrodes, and for this reason it was decided to perform temperature measurements on only one of the 2 fabricated wafers. Measurements were made at 5°C intervals for the $\Psi = 119°$ and $\Psi = 123°$ devices and at 10°C intervals for the remaining 5 devices. The reason for making measurements with higher temperature resolution for 2 of the devices was to accurately determine the turnover temperature because these orientations exhibit temperature compensation near room temperature. The normalized frequency variation for each device was calculated by:

$$\Delta f(T)/f_0 = \frac{f(T) - f(25°\text{C})}{f(25°\text{C})}. \tag{2}$$

Similarly, TCD was calculated by:

$$\text{TCD}(T) = \frac{-1}{f(T)} \frac{f(T+\varepsilon) - f(T-\varepsilon)}{2\varepsilon}, \tag{3}$$

where the minus sign in (3) results from the relation of TCD and the temperature coefficient of frequency, TCF $= -$TCD, and ε is a small temperature change, either 5 or 10°C, depending on the temperature interval used in the measurement. The 0.1°C precision in the measurement of temperature was high enough that the error in temperature measurements contributed a negligible amount to the uncertainty in the measured $\Delta f/f_0$ and TCD, so the uncertainties in these quantities were calculated by propagating the uncertainty in the measured frequencies.

TABLE I. SENSITIVITY OF SAWS TO THE 6 ELASTIC CONSTANTS.

	$\partial v_p/\partial C_{ij}$ (m s^{-1} Pa^{-1}) $\times 10^{-10}$						
	$\Psi = 0°$	$\Psi = 13°$	$\Psi = 48°$	$\Psi = 77°$	$\Psi = 119°$	$\Psi = 123°$	$\Psi = 170°$
C_{11}	4	4	4	3	10	6	1
C_{13}	−6	−4	−7	−6	−12	−8	−2
C_{14}	−190	−260	−260	−280	−51	4	−190
C_{33}	2	2	4	3	5	3	1
C_{44}	55	101	75	80	83	28	46
C_{66}	263	223	248	257	179	236	287

III. CALCULATED SAW PROPERTY UNCERTAINTY

The methods governing the calculation of LGT SAW phase velocity for electrically open and shorted surfaces, needed for the calculation of SAW properties including: v_p, TCD, K^2, PFA, acoustic diffraction, and wave polarization are described elsewhere [2], [11], [18] and will not be further discussed here. This section focuses on the estimation of uncertainty in the calculated v_p and TCD, based upon the uncertainties in the acoustic material constants used in the calculations and the sensitivity of the SAW along a specific orientation to the different material constants.

As a point group 32 crystal, LGT has 6 independent elastic constants, C_k, where the index k represents here the 6 elastic constants of LGT. If one considers only the influence of the elastic constants on the phase velocity error, this error is calculated by:

$$\delta_{\mathrm{vp}}^{\mathrm{C}} = \sqrt{\sum_k \left(\frac{\partial v_p}{\partial C_k}\right)^2 (\delta C_k)^2}. \tag{4}$$

The superscript 'C', in $\delta_{\mathrm{vp}}^{\mathrm{C}}$, is used to denote uncertainty in a calculated, as opposed to a measured, quantity. The exclusion of the piezoelectric constants in LGT SAW calculations influences the SAW phase velocity by less than 2% for all propagation directions in the $(90°, 23°, \Psi)$ plane. Because the piezoelectric and dielectric constants have such a reduced influence on the LGT SAW phase velocity calculation, the errors in the calculated v_p and TCD were assumed to depend solely on the errors in the elastic constants.

Unlike the case with bulk acoustic waves, for which analytical solutions for $\partial v_p/\partial C_{ij}$ exist, these quantities must normally be computed numerically for SAWs. These coefficients were determined for each of the 7 measured SAWs by calculating the SAW phase velocity using a slightly higher value for the 6 elastic constants. For example, to determine the sensitivity of a SAW to elastic constant C_{11}, this sensitivity was calculated by:

$$\frac{\partial v_p}{\partial C_{11}} = \frac{v_p(C_{11} \times 1.01) - v_p(C_{11})}{0.01 \times C_{11}}. \tag{5}$$

The partial derivatives were carried out by varying only one constant at a time, holding all others constant, for each of the 7 SAW propagation directions. The sensitivity of each of the modes to the 6 elastic constants is displayed in Table I.

The predicted TCD of the SAWs was calculated using the expression [19]:

$$\mathrm{TCD} = \frac{1}{l}\frac{dl}{dT} - \frac{1}{v_p}\frac{dv_p}{dT} = \mathrm{TCE} - \mathrm{TCV}, \tag{6}$$

where l is the SAW device's length and TCE and TCV are the temperature coefficients of expansion and velocity, respectively. From this expression, the uncertainty in the calculated TCD, $\delta_{\mathrm{TCD}}^{\mathrm{C}}$, can be written:

$$\delta_{\mathrm{TCD}}^{\mathrm{C}} = \sqrt{(\delta_{\mathrm{TCE}})^2 + \left(\frac{1}{{v_p}^2}\frac{dv_p}{dT}\right)^2 (\delta v_p)^2 + \left(\frac{1}{v_p}\right)^2 \left(\delta\frac{dv_p}{dT}\right)^2}, \tag{7}$$

where the uncertainty in the temperature derivative of phase velocity is calculated using the uncertainty in the temperature coefficients of the elastic constants, because the partial derivative of the phase velocity with respect to the elastic constants is a property of the crystal geometry:

$$\delta\frac{dv_p}{dT} = \sqrt{\sum_k \left(\frac{\partial v_p}{\partial C_k}\right)^2 \left(\delta\frac{dC_k}{dT}\right)^2}. \tag{8}$$

IV. RESULTS AND DISCUSSION

A. Room Temperature SAW Phase Velocities

For each of the 14 devices, the average frequency of repeated measurements was used to calculate the phase velocity of that device, and the standard error was used as the uncertainty. From the 5 measurements made on each device, one set of measurements on wafer A were discarded as outliers because the values were more than 2 standard deviations away from the mean of the 5 measurements. The phase velocities of each duplicate pair of devices with the same propagation direction were compared and agreed within the uncertainty of the measurements. The phase velocity for each propagation direction was then computed as the average of the velocities for each pair of

TABLE II. Measured and Predicted Room Temperature (25°C) SAW Properties.

	Measured			Predicted		
Ψ(°)	v_p[1] (m/s)	TCD (ppm/°C)	δ_{TCD} (ppm/°C)	v_p[2] (m/s)	TCD (ppm/°C)	δ_{TCD} (ppm/°C)
0	2445	−50	6	2449	−42	17
13	2335	−71	8	2338	−57	22
48	2311	−69	6	2310	−57	23
77	2327	−76	6	2326	−64	24
119	2730	−12	10	2720	4	7
123	2752	−6	10	2756	−12	7
170	2430	−52	6	2430	−48	17

[1]Measured v_p all ± 2 m/s.
[2]Predicted v_p all ± 10 m/s.

devices with the same orientation. The phase velocities determined for each of the 7 SAW propagation directions are displayed in Table II; all of them have an uncertainty of ±2 m/s or ∼0.1%. Table II also presents the predicted phase velocities, each of which has an uncertainty of ±10 m/s calculated using (4) and the reported uncertainties in [9]. There are 2 different sets of LGT elastic constants uncertainties determined by BAW measurements and reported in reference [9]: one determined analytically and another estimated through an optimization routine. The larger uncertainties determined by the optimization routine were used in this work to calculate the error in v_p. It should be noted that if the analytically determined elastic constants uncertainties are used instead, the uncertainty in the predicted SAW v_p is reduced to ∼3 m/s for each SAW, which is still in agreement with the measured values of v_p.

B. SAW Temperature Behavior

The TCD for each of the 7 orientations was determined from measurements between 10 and 130°C using (3). The TCDs predicted at room temperature are shown in Fig. 1 and in Table II and are based upon the constants published in [9]. Table II also presents the uncertainties for the predicted TCDs along the selected orientations calculated using (7). Uncertainties in the temperature derivatives of the elastic constants are critical for the estimation of uncertainty in temperature-related SAW propagation properties. The dC_{ij}/dT from [9] and the associated $\delta_{ij} = \delta(dC_{ij}/dT)$ which were used in this work are shown in Table III. It can be noted from Table II that the uncertainties in the measured TCD for the $\Psi = 119°$ and $\Psi = 123°$ SAWs are slightly larger than the uncertainties for the other 5 orientations, in part because of the smaller temperature intervals used in these 2 orientations measurements, which were necessary to more accurately determine the turnover temperature.

The predicted uncertainty in the TCD is dominated by the third term under the square root sign in (7). The uncertainty values in the predicted TCDs, δ^{C}_{TCD}, of the 7 SAW orientations studied here is almost entirely attributable to δ_{14}, which reflects: 1) the large v_p sensitivity to C_{14}, $\partial v_p/\partial C_{14}$, for most of the SAW orientations listed in Table I; and 2) the considerable value of δ_{14} which can be seen in Table III. Though $\partial v_p/\partial C_{66}$ is of the same order as $\partial v_p/\partial C_{14}$, δ_{66} is less than half as large as δ_{14}, leading to a reduced influence of C_{66} to δ^{C}_{TCD}. Because of the reduced sensitivity of v_p on C_{14} for $\Psi = 119°$ and $\Psi = 123°$, δ^{C}_{TCD} for these propagation directions is reduced to ∼1/3 with respect to the other 5 propagation directions.

TABLE III. Temperature Derivative of Elastic Constants.

C_{ij}	dC_{ij}/dT (MPa/°C)	δ_{ij} (MPa/°C)
C_{11}	−13.5	0.1
C_{13}	8.4	2
C_{14}	−4.9	2
C_{33}	−22.3	0.1
C_{44}	−0.05	0.3
C_{66}	0.6	0.8

The measured TCD for all 7 orientations was in agreement with values predicted by constants published in [9], within their associated uncertainties, over the entire temperature range measured. As an example, Fig. 3 shows the SAW $\Delta f/f_0$ temperature behavior and TCD for $\Psi = 170°$. The agreement between measured and calculated values for these propagation properties can be seen throughout the entire temperature range. Also plotted for comparison in Fig. 3 are the $\Delta f/f_0$ and TCD predicted using the material constants and temperature coefficients from [2], the only other reference which reported on the entire set of constants, including the thermal coefficients of expansion, needed to calculate the SAW propagation properties with temperature.

C. Zero TCD Orientations

As can be inferred from Fig. 1, the $\Psi = 119°$ and $\Psi = 123°$ SAW propagation directions lie in a region of space with electromechanical coupling nearly 7 times that of ST-X quartz and very low or zero calculated TCD. Fig. 4 presents the measured and predicted temperature behavior along one of these orientations, namely $\Psi = 123°$. From Fig. 4(a), it can be noted that the variation in frequency is less than 0.5 parts per thousand over the entire temperature range measured. The agreement between measured

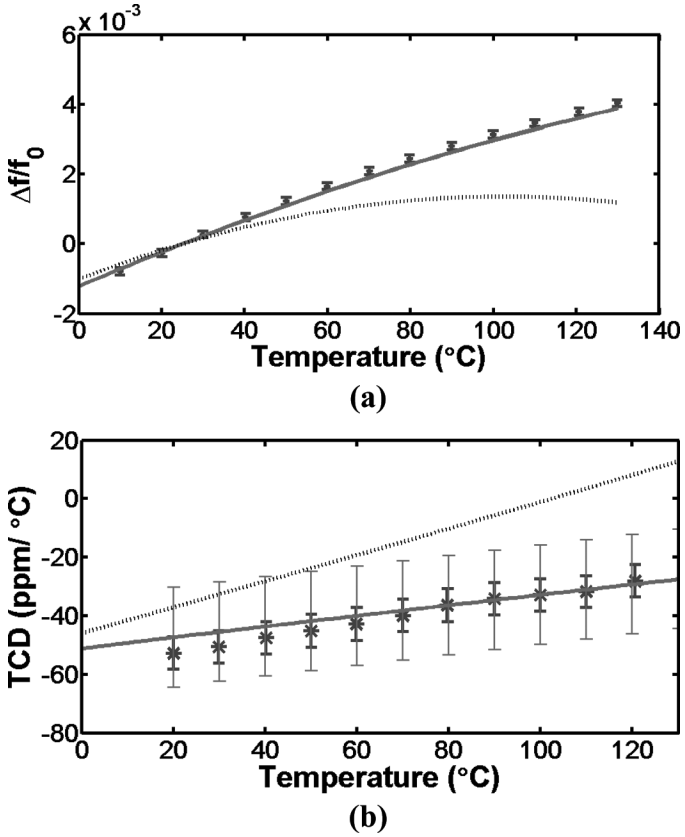

Fig. 3. (a) $\Delta f/f_0$ and (b) TCD for the $\Psi = 170°$ SAW. Asterisks denote experimental points. Solid and dashed traces are values predicted using constants in [9] and [2], respectively. Agreement between predicted temperature parameters and experiment are representative of all SAWs measured.

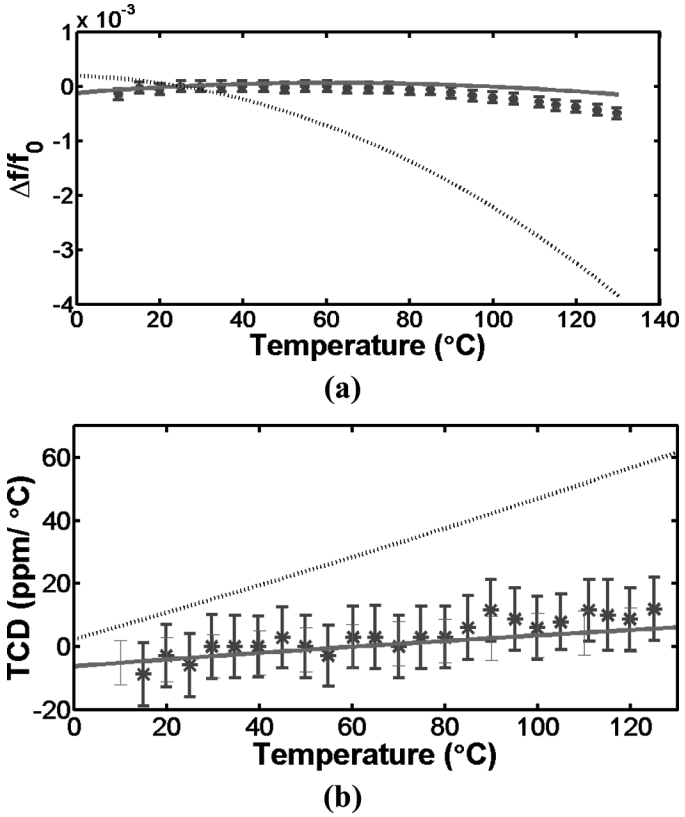

Fig. 4. (a) $\Delta f/f_0$ and (b) TCD for the $\Psi = 123°$ SAW. This mode exhibits zero TCD in the vicinity of room temperature and a normalized frequency variation of less than 5 parts per thousand over a 120°C temperature span. Asterisks denote experimental points. Solid and dashed traces are predicted values using constants in [9] and [2], respectively.

TCD (asterisks) and predicted TCD (solid line) is excellent over the entire temperature range measured. A linear fit (not shown) to the measured TCDs for the $\Psi = 123°$ SAW yields a value of zero TCD at 50°C. A similar case was found for the $\Psi = 119°$ mode, where the zero TCD identified by a linear fit to the data is at 60°C. As suggested by Fig. 1 and supported by measurements of the $\Psi = 119°$ and 123° propagation directions (Fig. 4 and Table II), SAWs along Euler angles $(90°, 23°, 110° < \Psi < 130°)$ and in the neighborhood of space defined by $(90° \pm \Delta, 23° \pm \Delta, 110° < \Psi < 130°)$ with Δ a variation around those angles, are very promising because of their low frequency variation with respect to temperature changes and their predicted coupling up to 0.75%.

V. Conclusions

The accuracy of a recently reported set of langatate material constants and temperature coefficients was investigated through the use of surface acoustic wave delay line measurements. The frequency response of devices aligned along 7 orientations within the $(90°, 23°, \Psi)$ plane were measured as a function of temperature. The room temperature phase velocities and the temperature coefficient of delay over a temperature range of 120°C were found to be in agreement with predictions within the uncertainty limits of both the measurements and predictions.

A method for estimating the uncertainty in calculated SAW propagation properties such as phase velocity and temperature coefficient of delay based upon uncertainties in the fundamental material constants was developed and discussed.

A new LGT plane with an orientation region exhibiting both predicted coupling of ~0.7% and temperature compensation around room temperature was uncovered. The orientation $(90°, 23°, 123°)$ in particular was verified to have less than 0.5 parts per thousand frequency variation over the entire temperature range measured (10°C to 130°C). The $(90°, 23°, 119°)$ and $(90°, 23°, 123°)$ orientations were found to have turnover temperatures at 60 and 50°C, respectively.

The SAW plane selected successfully validated the previously measured constants by the UMaine group for the temperature range between 10 to 130°C.

Acknowledgments

The authors gratefully acknowledge Mr. B. Meulendyk and Mr. P. Davulis of the Laboratory for Surface Sci-

ence & Technology at UMaine for their assistance in the SAW device fabrication and in the hours spent on sample preparation.

References

[1] B. Chai, J. L. Lefaucheur, Y. Y. Ji, and H. Qiu, "Growth and evaluation of large size LGS ($La_3Ga_5SiO_{14}$), LGN ($La_3Ga_{5.5}Nb_{0.5}O_{14}$) & LGT ($La_5Ga_{5.5}Ta_{0.5}O_{14}$) single crystals," in *Proc. 1998 IEEE Int. Frequency Control Symp.*, pp. 748–760.

[2] M. Pereira da Cunha, D. C. Malocha, E. L. Adler, and K. J. Casey, "Surface and pseudo surface acoustic waves in langatate: predictions and measurements," *IEEE Trans. Ultrason. Ferroelectr. Freq. Cont.*, vol. 49, pp. 1291–1299, Sep. 2002.

[3] Y. V. Pisarevsky, P. A. Senyushenkov, B. V. Mill, and N. A. Moiseeva, "Elastic, piezoelectric, dielectric properties of $La_3Ga_{5.5}Ta_{0.5}O_{14}$ single crystals," in *Proc. 1998 IEEE Int. Frequency Control Symp.*, pp. 742–747.

[4] J. Bohm, E. Chilla, C. Flannery, H. J. Frohlich, T. Hauke, R. B. Heimann, M. Hengst, and U. Straube, "Czochralski growth and characterization of piezoelectric single crystals with langasite structure: $La_3Ga_5SiO_{14}$ (LGS), $La_3Ga_{5.5}Nb_{0.5}O_{14}$ (LGN) and $La_3Ga_{5.5}Ta_{0.5}O_{14}$ (LGT) II. Piezoelectric and elastic properties," *J. Cryst. Growth*, vol. 216, pp. 293–298, 2000.

[5] N. Onozato, M. Adachi, and T. Karaki, "Surface acoustic wave properties of $La_3Ta_{0.5}Ga_{5.5}O_{14}$ single crystals," *Jpn. J. Appl. Phys.*, vol. 39, pp. 3028–3031, May 2000.

[6] J. Schreuer, "Elastic and piezoelectric properties of $La_3Ga_5SiO_{14}$ and $La_3Ga_{5.5}Ta_{0.5}O_{14}$: An application of resonant ultrasound spectroscopy," *IEEE Trans. Ultrason. Ferroelectr. Freq. Cont.*, vol. 49, pp. 1474–1479, Nov. 2002.

[7] D. C. Malocha, M. Pereira da Cunha, E. Adler, R. C. Smythe, S. Frederick, M. Chou, R. Helmbold, and Y. S. Zhou, "Recent measurements of material constants versus temperature for langatate, langanite, and langasite," in *Proc. 2000 IEEE Int. Frequency Control Symp.*, pp. 200–205.

[8] E. Chilla, C. M. Flannery, and H. J. Frohlich, "Elastic properties of langasite-type crystals determined by bulk and surface acoustic waves," *J. Appl. Phys.*, vol. 90, pp. 6084–6091, Dec. 2001.

[9] B. T. Sturtevant, P. M. Davulis, and M. Pereira da Cunha, "Pulse echo and combined resonance techniques: A full set of LGT acoustic wave constants and temperature coefficients," *IEEE Trans. Ultrason., Ferroelectr. Freq. Cont.*, vol. 56, pp. 788–797, Apr. 2009.

[10] J. A. Kosinski, "New piezoelectric substrates for SAW devices," *Int. J. High Speed Electron. Syst.*, vol. 10, no. 4, pp. 1017–1068, 2000.

[11] M. Pereira da Cunha and S. de Azevedo Fagundes, "Investigation of recent quartz-like materials for SAW applications," *IEEE Trans. Ultrason. Ferroelectr. Freq. Cont.*, vol. 46, pp. 1583–1590, Nov. 1999.

[12] J. Schreuer, C. Thybaut, M. Prestat, J. Stade, and E. Haussuhl, "Towards an understanding of the anomalous electromechanical behaviour of langasite and related compounds at high temperatures," in *Proc. 2003 IEEE Int. Ultrasonics Symp.*, pp. 196–199.

[13] R. Fachberger, E. Riha, E. Born, and P. Pongratz, "Homogeneity of langasite and langatate wafers for acoustic wave applications," in *Proc. 2003 IEEE Int. Ultrasonics Symp.*, pp. 100–109.

[14] T. R. Beaucage, E. P. Beenfeldt, S. A. Speakman, W. D. Porter, E. A. Payzant, and M. Pereira da Cunha, "Comparison of high temperature crystal lattice and bulk thermal expansion measurements of LGT single crystal," in *Proc. 2006 IEEE Int. Frequency Control Symp.*, pp. 658–663.

[15] P. M. Davulis, B. T. Sturtevant, S. I. Duy, and M. Pereira da Cunha, "Revisiting LGT dielectric constants and temperature coefficients up to 120 deg. C," in *Proc. 2007 Int. Ultrasonics Symp.*, pp. 1397–1400.

[16] L. D. Doucette, M. Pereira da Cunha, and R. J. Lad, "Precise orientation of single crystals by a simple X-ray diffraction rocking curve method," *Rev. Sci. Instr.*, vol. 76, art. no. 036106, 2005.

[17] B. T. Sturtevant, M. Pereira da Cunha, and R. J. Lad, "Determination of the absolute orientation of langatate crystals using X-ray diffraction," in *Proc. 2008 Int. Ultrasonics Symp.*, pp. 741–744.

[18] J. A. Cowperthwaite and M. Pereira da Cunha, "Optimal orientation function for SAW devices," in *Proc. 2003 IEEE Int. Frequency Control Symp.*, pp. 881–887.

[19] D. P. Morgan, *Surface-Wave Devices for Signal Processing*. New York: Elsevier, 1991.

Blake Sturtevant (S'06) was born in Waterville, Maine in 1981. In 2003, he received a B.A. degree in physics from Bowdoin College, Brunswick, Maine.

Since 2004, Mr. Sturtevant has been working toward the Ph.D. degree in physics at the University of Maine. His research is focused on the characterization of piezoelectric single crystals for acoustic wave applications.

Mr. Sturtevant has been a National Science Foundation IGERT trainee since 2005. He is a member of the IEEE and the American Physical Society (APS).

Mauricio Pereira da Cunha (S'88–M'95–SM'02) was born in Brazil in 1963. He received the Bachelor's degree and the Master's degree with Honors in electrical engineering, from the Escola Politécnica, Universidade de São Paulo in 1985 and 1989, respectively. His Master's thesis title is "Design and Implementation of a 70 MHz SAW Convolver." He received the Ph.D. degree, Dean's Honor List, from McGill University, Montreal, PQ, Canada, in electrical engineering in 1994. His Ph.D. thesis title is "SAW Propagation and Device Modeling on Arbitrarily Oriented Substrates."

Mauricio has worked with the Microwave Devices R&D Group at NEC (Nippon Electric Co.), Brazil, Laboratório de Microeletrônica, Escola Politécnica, Department of Electrical Engineering, Universidade de São Paulo, McGill University, Montreal, PQ, Canada, and SAWTEK Inc., Orlando, FL. He passed a sabbatical year at University of Central Florida, Consortium for Applied Acoustoelectronic Technology (CAAT), Orlando, FL, where he worked in cooperation with Piezotechnology Inc, on the characterization of new piezoelectric materials, namely langatate, langanite, and langasite, and with bulk and surface acoustic wave devices. Mauricio was a Professor in the Department of Electronic Engineering, Universidade de São Paulo until he joined the Department of Electrical and Computer Engineering at the University of Maine in 2001, where he presently holds the position of Associate Professor.

Dr. Pereira da Cunha is a member of the IEEE, Sigma Xi, and of the Brazilian Microwave Society (SBMO). He was elected to serve on the SBMO Administrative Committee from 1996 to 1999. He is a reviewer and an associate editor for the *IEEE Transactions on Ultrasonics, Ferroelectrics, and Frequency Control*, and he has been a member of the IEEE International Ultrasonics Symposium Technical Program Committee since 1997. He has served on the UFFC-Society Administrative Committee from 2002 to 2004, served as Technical Program Committee Chair for the IEEE 2007 Ultrasonics Symposium, in New York, NY, and is presently the Vice-President for Ultrasonics. He has more than 140 publications in the area of microwave acoustic propagation, acoustic wave material properties, bulk and surface acoustic wave modeling and devices, and sensors.